Accuracy of the Quantum Regression Theorem for Photon Emission from a Quantum Dot

M. Cosacchi[●],[1] T. Seidelmann[●],[1] M. Cygorek[●],[2] A. Vagov[●],[1,3] D. E. Reiter[●],[4] and V. M. Axt[1]

[1]*Theoretische Physik III, Universität Bayreuth, 95440 Bayreuth, Germany*
[2]*Heriot-Watt University, Edinburgh EH14 4AS, United Kingdom*
[3]*ITMO University, St. Petersburg 197101, Russia*
[4]*Institut für Festkörpertheorie, Universität Münster, 48149 Münster, Germany*

The quantum regression theorem (QRT) is the most widely used tool for calculating multitime correlation functions for the assessment of quantum emitters. It is an approximate method based on a Markov assumption for environmental coupling. In this Letter we quantify properties of photons emitted from a single quantum dot coupled to phonons. For the single-photon purity and the indistinguishability, we compare numerically exact path-integral results with those obtained from the QRT. It is demonstrated that the QRT systematically overestimates the influence of the environment for typical quantum dots used in quantum information technology.

To be used as photon sources for quantum information technology [1,2], semiconductor quantum dots (QDs) must deliver photons with high-quality characteristics such as a high brightness, a perfect single-photon purity, and indistinguishability. However, due to the electron-phonon interaction in QDs these quantities can be degraded [3,4]. In the current race for the perfect single-photon source [5,6] with achieved purities and indistinguishabilities close to unity [4,7–12], it is crucial to understand the influence of the phonon-induced dephasing on the properties of emitted photons. The coupling to environmental phonons has been shown to lead to several important phenomena like the phonon sidebands [13,14], damping of Rabi oscillations [15–19], and the possibility for a dynamic decoupling of electronic and phononic subsystems [20,21], or degradation of photon properties [22].

The quantum regression theorem (QRT) known from quantum optics is probably the most widely used standard tool to investigate the above photon properties [23]. In essence, the QRT prescribes to calculate the two- (or multi-) time correlation functions using the same dynamical equation for both the (real-) time and the delay-time arguments, which is used to determine the time evolution of the single-time correlations. Solving an initial value problem for the delay-time propagation as done in the QRT disregards the memory that has build up until the start of the propagation, and thus, the use of the QRT may become critical when used for non-Markovian dynamics. With the help of the QRT, multitime correlation functions yielding, e.g., the purity and indistinguishability can be deduced. The QRT can be extended such that it also accounts for the electron-phonon interaction [24–28]. For our current study it is most important that phonons are known to induce non-Markovian dynamics [24,26,29–32] which provides a

situation where the QRT may come to its limits [33–37]. Because the QRT is an approximation it is not always clear, whether the assumptions made in the derivation are fulfilled.

Testing the limits of the QRT has recently become possible by a path-integral approach to calculate multitime photon correlation functions [38]. This approach is numerically exact meaning that the time-dependent solution to the many-body Hamiltionian model is obtained without any further approximations, and thus the phonon influence including its non-Markovian part is fully taken into account [39–41]. The accuracy of the result is controlled by choosing an appropriate time discretization and memory length.

In this Letter, we explore the limits of the QRT approximation for calculating multitime correlation functions using a QD coupled to phonons as an example. To compare numerically exact results with the QRT approximation in the most transparent way, we implement the QRT directly within the path-integral method. Since apart from the QRT no further approximations are involved, this approach offers a direct way to evaluate the influence of the QRT on the multitime correlations. Details of the implementations are found in the Supplemental Material [42].

We demonstrate that the QRT systematically overestimates the phonon impact on the indistinguishability, in particular for standard GaAs QDs relevant for technological applications [51–58]. We show that this is connected to the non-Markovian part of the dynamics. In contrast, the QRT yields quantitatively correct results for the purity.

We consider a model where a two-level QD can emit photons and interacts with environmental longitudinal acoustic (LA) phonons [14,32,59]. For the calculations we consider GaAs QDs of radius 3 nm and standard material parameters for the phonon coupling with the

100402-1

exception that we introduce a scaling factor λ modifying the overall coupling amplitude. Details of the model are found in the Supplemental Material [42]. We assume that this scaling is a variable in the interval $\lambda \in [0, 10]$, where 0 means the absence of phonons, 1 corresponds to the GaAs QDs, and larger values allow us to explore strongly coupled QD-phonon systems [39,60]. Larger couplings $1 < \lambda \leq 10$ can be found in piezoelectric materials like GaN [61]. We further account for the radiative decay of the QD exciton by introducing a Lindblad superoperator, setting the radiative decay rate to $\gamma = 1$ ns^{-1}. The QD is excited by an external laser pulse with a Gaussian envelope. We consider a resonant [62] excitation scheme with a π pulse of 3 ps length (full width at half maximum) [63] to prepare the excited state in the QD [7,28]. Using this model, we can then calculate the photonic properties.

The single-photon purity $\mathcal{P}$ is defined as

$$\mathcal{P} = 1 - p \quad \text{with} \quad p = \frac{\int_{-T_{\text{Pulse}}/2}^{T_{\text{Pulse}}/2} d\tau \, G^{(2)}(\tau)}{\int_{T_{\text{Pulse}}/2}^{3T_{\text{Pulse}}/2} d\tau \, G^{(2)}(\tau)}. \quad (1)$$

T_{Pulse} is the separation of the pulses in the excitation pulse train, and

$$G^{(2)}(\tau) := \lim_{T \to \infty} \frac{1}{T} \int_{-T}^{T} dt \, G^{(2)}(t, \tau), \quad (2a)$$

$$G^{(2)}(t, \tau) := \langle \sigma_X^\dagger(t) \sigma_X^\dagger(t + \tau) \sigma_X(t + \tau) \sigma_X(t) \rangle \quad (2b)$$

with σ_X describing the QD transition from the excited to the ground state. $\mathcal{P}$ is a measure for the single-photon component of the photonic state [1,7,8,64–68]. It is measured using a Hanbury Brown-Twiss setup [69], which is a coincidence measurement and can thus be modeled with a second-order two-time correlation function $G^{(2)}(\tau)$. $\mathcal{P} = 1$ implies a perfect single-photon purity. The quantity has no lower bound, $-\infty < \mathcal{P} \leq 1$, since p can be larger than 1 in the case of bunching instead of antibunching behavior.

The indistinguishability $\mathcal{I}$ of two successively emitted photons is obtained as

$$\mathcal{I} = 1 - p_{\text{HOM}} \quad \text{with} \quad p_{\text{HOM}} = \frac{\int_{-T_{\text{Pulse}}/2}^{T_{\text{Pulse}}/2} d\tau \, G_{\text{HOM}}^{(2)}(\tau)}{\int_{T_{\text{Pulse}}/2}^{3T_{\text{Pulse}}/2} d\tau \, G_{\text{HOM}}^{(2)}(\tau)}$$

$$(3)$$

with the correlation functions [28,70,71]

$$G_{\text{HOM}}^{(2)}(\tau) := \lim_{T \to \infty} \frac{1}{T} \int_{-T}^{T} dt \, G_{\text{HOM}}^{(2)}(t, \tau) \quad (4a)$$

$$G_{\text{HOM}}^{(2)}(t, \tau) := \frac{1}{2} [\langle \sigma_X^\dagger(t) \sigma_X(t) \rangle \langle \sigma_X^\dagger(t + \tau) \sigma_X(t + \tau) \rangle$$

$$- |\langle \sigma_X^\dagger(t + \tau) \sigma_X(t) \rangle|^2 + G^{(2)}(t, \tau)], \quad (4b)$$

where the last term in Eq. (4b) accounts for nonunity single-photon purities. This quantity is measured in a Hong-Ou-Mandel setup [72]. Perfect indistinguishability corresponds to $\mathcal{I} = 1$, and using the definition Eq. (4b) it is bounded by $0.5 \leq \mathcal{I} \leq 1$ [71]. We note that other definitions of $\mathcal{I}$ are often used which are not applicable when the single-photon purity deviates from unity and where the lower bound is 0 rather than 0.5 [22,73].

The brightness $\mathcal{B}$ of a photon source is defined as the number of photons emitted per excitation laser pulse [8]. It is given as [28,74]

$$\mathcal{B} := \gamma \int_{t_0 - T_{\text{Pulse}}/2}^{t_0 + T_{\text{Pulse}}/2} dt \, \langle \sigma_X^\dagger(t) \sigma_X(t) \rangle, \quad (5)$$

where t_0 is the center time of the pulse and $0 \leq \mathcal{B} \leq \gamma T_{\text{Pulse}}$. A value of $\mathcal{B}$ of 100% corresponds to the ideal case of a delta-pulse excitation.

To calculate these quantities we use the path-integral method both without and with the QRT. The path-integral method propagates the augmented density matrix that contains the information about the memory induced by the environment to the QD dynamics. Since the phonon-induced memory depth is finite, a memory window is formed in each time step. To implement the QRT, the augmented density matrix is traced over all memory-related variables at the end of the t propagation to yield a new initial reduced density matrix before the subsequent τ propagation. Thus, the accumulated phonon memory is discarded for the τ propagation. Therefore, the τ propagation becomes independent from the past evolution in t, which is the central assumption of the QRT. We have checked the validity of this approach by comparing our results with a standard implementation of the QRT as discussed in Ref. [26] and verify the finding therein that the QRT yields the phonon sidebands in emission spectra on the energetically wrong side, cf., Fig. 2 in the Supplemental Material [42].

Using the path-integral method, we calculate the photon properties $\mathcal{P}, \mathcal{I},$ and $\mathcal{B}$ for a wide parameter range as shown in Fig. 1, which displays the results using the path-integral approach without the QRT approximation. In the phonon-free case, $\lambda = 0$, the excitation of the QD leads to a near-optimal single-photon source with $\mathcal{P} = 99.76\%$, $\mathcal{I} = 99.76\%$, and $\mathcal{B} = 99.82\%$. Slight deviations $(< 0.3\%)$ from the perfect source can be traced back to the finite pulse length.

While the single-photon purity is close to unity for the entire parameter range under consideration, for a finite phonon scaling λ, the indistinguishability rapidly deteriorates with rising temperature T, such that for $\lambda = 1$ it falls below 70% when $T > 30$ K. For large phonon scalings, the indistinguishability cannot exceed 60% even at $T = 4$ K. At higher temperatures and for large phonon scaling, the indistinguishability decreases to its lowest possible value of
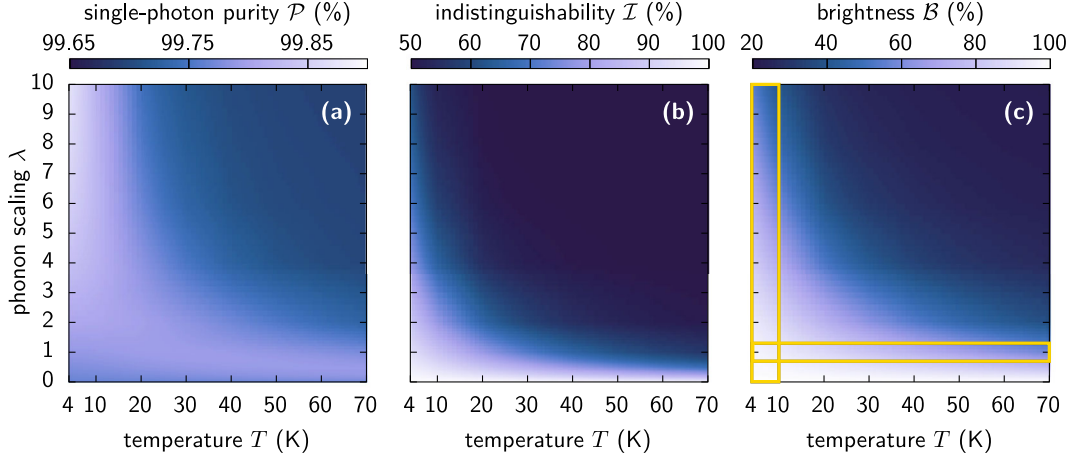
FIG. 1. The single-photon purity (a), the indistinguishability of two successively emitted photons (b), and their brightness (c) in a two-level QD for a temperature range between 4 and 70K and phonon scalings from 0 to 10. Yellow rectangles in panel (c) mark the physically important parameter regime of GaAs around $\lambda = 1$ for different temperatures and different phonon scalings for temperatures below 10K.

50%. Nonetheless, the corresponding brightness is non-vanishing, such that the QD becomes a source of distinguishable single photons in this regime of higher temperatures and stronger QD-phonon coupling.

We have marked the most physically relevant regions with yellow boxes in Fig. 1(c). They correspond to the low-temperature regime in which experiments are typically conducted for different QD materials from GaAs to GaN modeled here by different scalings λ (vertical box) as well as over a temperature range between liquid helium and nitrogen temperatures (horizontal box) for GaAs ($\lambda = 1$). In the parameter range of highest interest, i.e., where the boxes overlap at $\lambda = 1$ and $T = 4$ K, we find $\mathcal{P} = 99.79\%$, $\mathcal{I} = 93.16\%$, and $\mathcal{B} = 96.75\%$.

We now evaluate how the QRT approximation changes these results. It is usually conjectured that the QRT might fail when the dynamics is non-Markovian, i.e., when memory effects are nonnegligible [34,35]. Furthermore, there is a class of environmental couplings for which the QRT cannot be accurately applied, even when the single-time dynamics is Markovian [36]. In order to describe the contribution of the memory effects quantitatively, we consider a non-Markovianity measure for our system.

In contrast to classical Markovian stochastic processes, in open quantum systems there is no single definition of Markovianity (or non-Markovianity) that is agreed upon. Rather, there are different measures that capture different aspects of Markovian quantum dynamics [75–81], one of
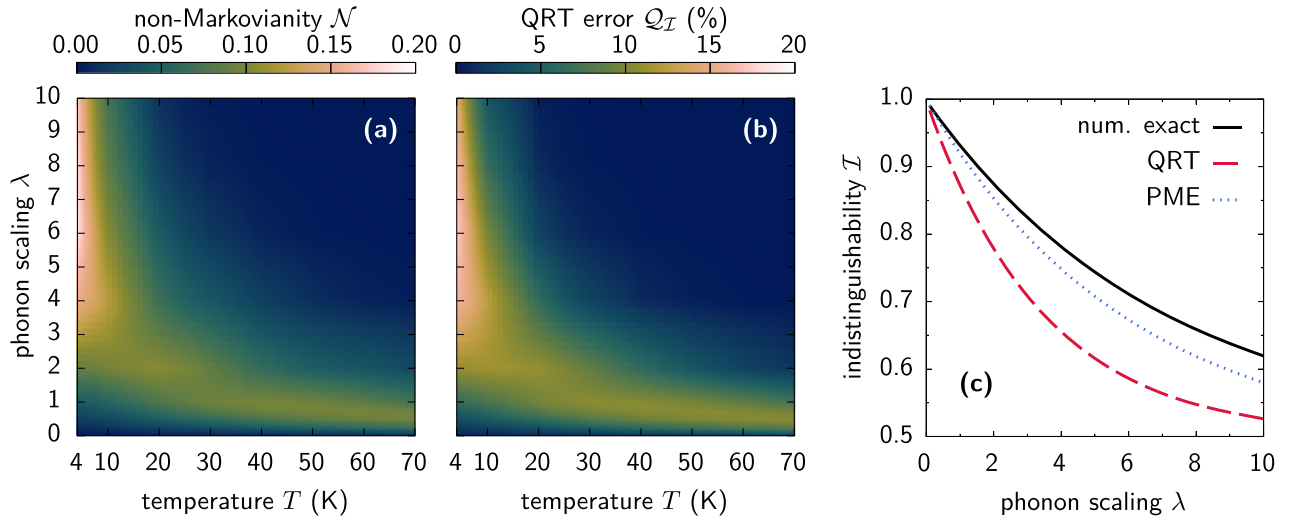
FIG. 2. The non-Markovianity measure $\mathcal{N}$ (a) and the relative error $\mathcal{Q}_\mathcal{I}$ for the indistinguishability (b) as a function of temperature T and phonon scaling λ. (c) The indistinguishability as a function of the phonon scaling parameter l at 4K, calculated with the numerically exact path-integral method (num. exact), by using the QRT in the lab frame (QRT), and by applying the QRT in the polaron transformed frame within the PME approach (PME).

which is the trace distance measure. The trace distance between two states described by the reduced density matrices ρ_1 and ρ_2 is defined as

$$D[\rho_1(t),\rho_2(t)] := \frac{1}{2}||\rho_1(t) - \rho_2(t)||_1 = \frac{1}{2}\sum_k |x_k(t)|, \quad (6)$$

where $x_k(t)$ are the eigenvalues of the difference matrix $\rho_1(t) - \rho_2(t)$. In our case, ρ_1 and ρ_2 correspond to arbitrary states chosen on the Bloch sphere of the two-level QD.

For Markovian dynamics, this quantity is a contraction:

$$\frac{d}{dt}D[\rho_1(t),\rho_2(t)] \le 0. \quad (7)$$

The intuitive explanation for this behavior lies in the loss of information in a Markovian system: two originally distinct states monotonically lose their distinguishability over time. Only in a non-Markovian system, information can flow back from the environment to the system, making the trace distance a nonmonotonic function of time. Therefore, the non-Markovianity of a system can be quantified as [26,36,75]

$$\mathcal{N} := \max_{\rho_1,\rho_2} \int_{\Omega_+} \frac{d}{dt}D[\rho_1(t),\rho_2(t)]dt. \quad (8)$$

Ω_+ is the union of the intervals on which $(d/dt)D[\rho_1(t),\rho_2(t)] > 0$. The maximum is taken over all pairs of possible initial states. Fortunately, only the subset of those states, which are orthogonal to each other, needs to be considered [82]. For our two-level system, this means that the corresponding Bloch sphere needs to be sampled only for pairs of opposing points on its surface.

While $\mathcal{N} = 0$ implies Markovianity, it is important to realize that $\mathcal{N} \ne 0$ implies that the underlying dynamical map is *indivisible* [36]. Therefore, the measure $\mathcal{N}$ captures the appearance of memory effects in the dynamics of the system, which is a fundamental aspect of non-Markovianity both in classical stochastic processes and open quantum systems.

To quantify the deviations introduced by the QRT, we define the relative error of evaluating a target quantity M using the QRT as a measure for the validity of the QRT with respect to M:

$$\mathcal{Q}_M = \left| \frac{M - M_{\mathrm{QRT}}}{M} \right|, \quad (9)$$

where M is calculated numerically exact and M_{QRT} using the QRT.

The QRT states that the same dynamical map that is used to evolve the density matrix and, in extension, expectation values of any subsystem operator, can be used for the time evolution of multitime correlation functions used in Eqs. (2b) and (4b). In particular, the differential equation propagating the density matrix in the real time t is reused for the propagation in the delay time τ [83,84]. This assumption presumes that the initial factorization of subsystem and environment common in the description of open quantum systems is also used at the beginning of the τ dynamics. In other words, this factorization is assumed for every t.

Now, we examine the impact of the QRT approximation on the photon source characteristics considered above. The non-Markovianity measure $\mathcal{N}$ and the relative error $\mathcal{Q}_{\mathcal{I}}$ for the indistinguishability are depicted in Figs. 2(a) and 2(b) as a function of T and λ. We see large values of $\mathcal{N}$ and $\mathcal{Q}_{\mathcal{I}}$, in particular, in the physically relevant parameter regimes, i.e., at $\lambda = 1$ and low temperatures. The largest $\mathcal{N}$ is found for $\lambda > 1$ and $T < 10$ K [cf., Fig. 2(a)], where the error introduced by using the QRT also rises up to roughly 18%. This behavior can be related to the connection between Markovianity and the QRT. Interestingly, there are also parameter ranges with a nonzero $\mathcal{N}$, where the QRT error is insignificant, e.g., at $\lambda = 10$ and $T = 20$ K, where $\mathcal{N} = 0.0125$, while $\mathcal{Q}_{\mathcal{I}} = 0.3\%$. This means that there are parameter sets where the QRT approximation is valid to a better degree than a Markovian description. This is unexpected since the former imposes more restrictive conditions on the system dynamics: for the QRT to hold, the subsystem and environment have to factorize for all times t, not only at the initial time. In the entire parameter regime considered here, the QRT overestimates the phonon influence on $\mathcal{I}$, that is $\mathcal{I} > \mathcal{I}_{\mathrm{QRT}}$, cf., Fig. 2(c) for a slice at 4K.

In contrast, the error $\mathcal{Q}_{\mathcal{P}}$ introduced by the QRT to the single-photon purity is negligible, and the brightness is unaffected by the QRT, since its definition in Eq. (5) contains only expectation values at a single time. Surprisingly, $\mathcal{Q}_{\mathcal{P}}$ is also extraordinarily small, being on the order of 10^{-4} for all considered parameter values (not shown), in contrast to $\mathcal{Q}_{\mathcal{I}}$.

In order to understand this, we examine the multitime correlation functions. While the purity contains only the second-order correlation $G^{(2)}(t,\tau)$, the indistinguishability also includes the correlation $G^{(1)}(t,\tau) := \langle \sigma_X^\dagger(t+\tau)\sigma_X(t) \rangle$. In $G^{(2)}(t,\tau)$ the operators $\sigma_X^\dagger$ and σ_X appear in pairs at each time t and $t+\tau$, respectively, hence modeling intensity-intensity correlation measurements, i.e., the correlation between occupations. In $G^{(1)}(t,\tau)$ on the other hand, $\sigma_X^\dagger$ and σ_X appear as stand-alone operators for each time argument in $G^{(1)}(t,\tau)$. Therefore, this function correlates coherences rather than occupations. Because the coupling to the LA phonon environment has a stronger impact on coherences than on occupations, it becomes clear why the approximations introduced by the QRT have a significantly stronger impact on $\mathcal{I}$ than on $\mathcal{P}$.

This finding implies two consequences: first, the single-photon purity can be calculated using the QRT with

negligible error, even for those parameters, where the dynamics is clearly non-Markovian according to the measure $\mathcal{N}$ [cf., Fig. 2(a)]. Second, one cannot use $\mathcal{Q}_{\mathcal{P}}$ as a *general* measure for the validity of the QRT. Using it in such a way would imply the validity of the QRT, which is misleading since in the same parameter regimes considered, the indistinguishability is off by up to 18% when evaluating with the QRT.

Finally, we analyze the frame dependence of the QRT by applying it in a polaron transformed frame. This technique is widely used in the polaron master equation approach (PME) [85–87] (see also Supplemental Material [42]). In Fig. 2(c), the indistinguishability is shown for a varying phonon scaling parameter λ at $T = 4$ K. The numerically exact result (black solid line) is compared with the calculation using the QRT in the lab frame (red dashed line) and the PME approach applying the QRT in the polaron frame (blue dotted line). While all methods yield qualitatively the same dependency, the PME produces results closer to the numerically exact calculation. While the largest relative error encountered in the slice shown in Fig. 2(c) is 18% for the QRT in the lab frame (red dashed line), it is only 6% when the QRT is applied in the polaron frame within the PME. The better performance of the PME is expected because due to the transformation to the polaron frame a variety of, but not all, non-Markovian effects are captured. Therefore, changing the frame improves the usage of the QRT, but still a significant systematic overestimation of phonon effects on the photon indistinguishability is obtained.

In summary, assessing the validity of the commonly used QRT is dependent on the target quantity that is calculated. In particular, there is no single measure by which the validity of the QRT could be estimated for all possible figures of merit derived from multitime correlation functions. Using a numerically exact path-integral method to calculate the properties of photons emitted from a QD coupled to LA phonons enabled us to explore the boundaries of the QRT, showing that the phonon effect on photon indistinguishability is systematically overestimated by the QRT, while the purity can be safely calculated using the QRT. Unlike what is found for other systems [36], the QRT induces errors in the photon emission from QDs typically only when the dynamics is non-Markovian. Though we show that due to the phonons the photon properties are limited close to but below unity in typical cases, there is still room for improvement, e.g., by placing the QD in a cavity. Furthermore, our results should be applicable to a broad range of physical two-level systems, such as defects in diamonds [88–93], silicon [94,95], hexagonal boron nitride [96,97], or other solid-state emitters [98] coupled to a continuum of environmental oscillators.

[1] P. Michler, A. Kiraz, C. Becher, W. V. Schoenfeld, P. M. Petroff, L. Zhang, E. Hu, and A. Imamoglu, A quantum dot single-photon turnstile device, Science **290**, 2282 (2000).

[2] P. Senellart, G. Solomon, and A. White, High-performance semiconductor quantum-dot single-photon sources, Nat. Nanotechnol. **12**, 1026 (2017).

[3] S. Gerhardt, J. Iles-Smith, D. P. S. McCutcheon, Y.-M. He, S. Unsleber, S. Betzold, N. Gregersen, J. Mørk, S. Höfling, and C. Schneider, Intrinsic and environmental effects on the interference properties of a high-performance quantum dot single-photon source, Phys. Rev. B **97**, 195432 (2018).

[4] B.-Y. Wang, E. V. Denning, U. M. Gür, C.-Y. Lu, and N. Gregersen, Micropillar single-photon source design for simultaneous near-unity efficiency and indistinguishability, Phys. Rev. B **102**, 125301 (2020).

[5] H. Vural, S. L. Portalupi, and P. Michler, Perspective of self-assembled ingaas quantum-dots for multi-source quantum implementations, Appl. Phys. Lett. **117**, 030501 (2020).

[6] S. Thomas and P. Senellart, The race for the ideal single-photon source is on, Nat. Nanotechnol. **16**, 367 (2021).

[7] X. Ding, Y. He, Z.-C. Duan, N. Gregersen, M.-C. Chen, S. Unsleber, S. Maier, C. Schneider, M. Kamp, S. Höfling, C.-Y. Lu, and J.-W. Pan, On-Demand Single Photons with High Extraction Efficiency and Near-Unity Indistinguishability from a Resonantly Driven Quantum Dot in a Micropillar, Phys. Rev. Lett. **116**, 020401 (2016).

[8] N. Somaschi *et al.*, Near-optimal single-photon sources in the solid state, Nat. Photonics **10**, 340 (2016).

[9] Y. Arakawa and M. J. Holmes, Progress in quantum-dot single photon sources for quantum information technologies: A broad spectrum overview, Appl. Phys. Rev. **7**, 021309 (2020).

[10] N. Tomm, A. Javadi, N. O. Antoniadis, D. Najer, M. C. Löbl, A. R. Korsch, R. Schott, S. R. Valentin, A. D. Wieck, A. Ludwig, and R. J. Warburton, A bright and fast source of coherent single photons, Nat. Nanotechnol. **16**, 399 (2021).

[11] S. E. Thomas, M. Billard, N. Coste, S. C. Wein, Priya, H. Ollivier, O. Krebs, L. Tazaïrt, A. Harouri, A. Lemaitre, I. Sagnes, C. Anton, L. Lanco, N. Somaschi, J. C. Loredo, and P. Senellart, Bright Polarized Single-Photon Source Based on a Linear Dipole, Phys. Rev. Lett. **126**, 233601 (2021).

[12] L. Zhai, G. N. Nguyen, C. Spinnler, J. Ritzmann, M. C. Lbl, A. D. Wieck, A. Ludwig, A. Javadi, and R. J. Warburton, Quantum interference of identical photons from remote quantum dots, arXiv:2106.03871.

[13] L. Besombes, K. Kheng, L. Marsal, and H. Mariette, Acoustic phonon broadening mechanism in single quantum dot emission, Phys. Rev. B **63**, 155307 (2001).

[14] B. Krummheuer, V. M. Axt, and T. Kuhn, Theory of pure dephasing and the resulting absorption line shape in semiconductor quantum dots, Phys. Rev. B **65**, 195313 (2002).

[15] J. Förstner, C. Weber, J. Danckwerts, and A. Knorr, Phonon-Assisted Damping of Rabi Oscillations in Semiconductor Quantum Dots, Phys. Rev. Lett. **91**, 127401 (2003).

[16] P. Machnikowski and L. Jacak, Resonant nature of phonon-induced damping of Rabi oscillations in quantum dots, Phys. Rev. B **69**, 193302 (2004).

[17] A. Vagov, V. M. Axt, T. Kuhn, W. Langbein, P. Borri, and U. Woggon, Nonmonotonous temperature dependence of the

initial decoherence in quantum dots, Phys. Rev. B **70**, 201305(R) (2004).

[18] A. Vagov, M. D. Croitoru, V. M. Axt, T. Kuhn, and F. M. Peeters, Nonmonotonic Field Dependence of Damping and Reappearance of Rabi Oscillations in Quantum Dots, Phys. Rev. Lett. **98**, 227403 (2007).

[19] A. J. Ramsay, A. V. Gopal, E. M. Gauger, A. Nazir, B. W. Lovett, A. M. Fox, and M. S. Skolnick, Damping of Exciton Rabi Rotations by Acoustic Phonons in Optically Excited InGaAs/GaAs Quantum Dots, Phys. Rev. Lett. **104**, 017402 (2010).

[20] T. Kaldewey, S. Lüker, A. V. Kuhlmann, S. R. Valentin, J.-M. Chauveau, A. Ludwig, A. D. Wieck, D. E. Reiter, T. Kuhn, and R. J. Warburton, Demonstrating the decoupling regime of the electron-phonon interaction in a quantum dot using chirped optical excitation, Phys. Rev. B **95**, 241306(R) (2017).

[21] S. Lüker and D. E. Reiter, A review on optical excitation of semiconductor quantum dots under the influence of phonons, Semicond. Sci. Technol. **34**, 063002 (2019).

[22] J. Iles-Smith, D. P. S. McCutcheon, A. Nazir, and J. Mørk, Phonon scattering inhibits simultaneous near-unity efficiency and indistinguishability in semiconductor single-photon sources, Nat. Photonics **11**, 521 (2017).

[23] H. Breuer and F. Petruccione, *The Theory of Open Quantum Systems* (Oxford University Press, New York, 2002).

[24] P. Kaer, P. Lodahl, A.-P. Jauho, and J. Mork, Microscopic theory of indistinguishable single-photon emission from a quantum dot coupled to a cavity: The role of non-Markovian phonon-induced decoherence, Phys. Rev. B **87**, 081308(R) (2013).

[25] K. Roy-Choudhury and S. Hughes, Quantum theory of the emission spectrum from quantum dots coupled to structured photonic reservoirs and acoustic phonons, Phys. Rev. B **92**, 205406 (2015).

[26] D. P. S. McCutcheon, Optical signatures of non-Markovian behavior in open quantum systems, Phys. Rev. A **93**, 022119 (2016).

[27] J. Iles-Smith, D. P. S. McCutcheon, J. Mørk, and A. Nazir, Limits to coherent scattering and photon coalescence from solid-state quantum emitters, Phys. Rev. B **95**, 201305(R) (2017).

[28] C. Gustin and S. Hughes, Pulsed excitation dynamics in quantum-dot–cavity systems: Limits to optimizing the fidelity of on-demand single-photon sources, Phys. Rev. B **98**, 045309 (2018).

[29] P. Kaer, T. R. Nielsen, P. Lodahl, A.-P. Jauho, and J. Mørk, Non-Markovian Model of Photon-Assisted Dephasing by Electron-Phonon Interactions in a Coupled Quantum-Dot-Cavity System, Phys. Rev. Lett. **104**, 157401 (2010).

[30] D. P. S. McCutcheon and A. Nazir, Quantum dot Rabi rotations beyond the weak exciton–phonon coupling regime, New J. Phys. **12**, 113042 (2010).

[31] A. Carmele and S. Reitzenstein, Non-Markovian features in semiconductor quantum optics: Quantifying the role of phonons in experiment and theory, Nanophotonics **8**, 655 (2019).

[32] D. E. Reiter, T. Kuhn, and V. M. Axt, Distinctive characteristics of carrier-phonon interactions in optically driven semiconductor quantum dots, Adv. Phys. **4**, 1655478 (2019).

[33] T. Renger and R. A. Marcus, On the relation of protein dynamics and exciton relaxation in pigmentprotein complexes: An estimation of the spectral density and a theory for the calculation of optical spectra, J. Chem. Phys. **116**, 9997 (2002).

[34] H.-P. Breuer, E.-M. Laine, J. Piilo, and B. Vacchini, Colloquium: Non-Markovian dynamics in open quantum systems, Rev. Mod. Phys. **88**, 021002 (2016).

[35] I. de Vega and D. Alonso, Dynamics of non-Markovian open quantum systems, Rev. Mod. Phys. **89**, 015001 (2017).

[36] G. Guarnieri, A. Smirne, and B. Vacchini, Quantum regression theorem and non-Markovianity of quantum dynamics, Phys. Rev. A **90**, 022110 (2014).

[37] A. Kurt, Two-time correlation functions beyond quantum regression theorem: Effect of external noise, Quantum Inf. Process. **20**, 238 (2021).

[38] M. Cosacchi, M. Cygorek, F. Ungar, A. M. Barth, A. Vagov, and V. M. Axt, Path-integral approach for nonequilibrium multitime correlation functions of open quantum systems coupled to Markovian and non-Markovian environments, Phys. Rev. B **98**, 125302 (2018).

[39] A. Vagov, M. D. Croitoru, M. Glässl, V. M. Axt, and T. Kuhn, Real-time path integrals for quantum dots: Quantum dissipative dynamics with superohmic environment coupling, Phys. Rev. B **83**, 094303 (2011).

[40] A. M. Barth, A. Vagov, and V. M. Axt, Path-integral description of combined Hamiltonian and non-Hamiltonian dynamics in quantum dissipative systems, Phys. Rev. B **94**, 125439 (2016).

[41] M. Cygorek, A. M. Barth, F. Ungar, A. Vagov, and V. M. Axt, Nonlinear cavity feeding and unconventional photon statistics in solid-state cavity QED revealed by many-level real-time path-integral calculations, Phys. Rev. B **96**, 201201(R) (2017).

[42] See Supplemental Material at http://link.aps.org/supplemental/10.1103/PhysRevLett.127.100402 for a complete definition of our model, in particular the phonon coupling, and a detailed explanation of the numerical procedure. Additionally, further details on the QRT in a polaron transformed frame are presented. It includes Refs. [43–50] in addition to other references already cited in the main text.

[43] P. Borri, W. Langbein, S. Schneider, U. Woggon, R. L. Sellin, D. Ouyang, and D. Bimberg, Ultralong Dephasing Time in InGaAs Quantum Dots, Phys. Rev. Lett. **87**, 157401 (2001).

[44] P. Machnikowski, V. M. Axt, and T. Kuhn, Quantum-information encoding in dressed qubits, Phys. Rev. A **75**, 052330 (2007).

[45] M. Florian, P. Gartner, C. Gies, and F. Jahnke, Phonon-mediated off-resonant coupling effects in semiconductor quantum-dot lasers, New J. Phys. **15**, 035019 (2013).

[46] A. Nysteen, P. Kaer, and J. Mork, Proposed Quenching of Phonon-Induced Processes in Photoexcited Quantum Dots due to Electron-Hole Asymmetries, Phys. Rev. Lett. **110**, 087401 (2013).

[47] D. P. S. McCutcheon and A. Nazir, Model of the Optical Emission of a Driven Semiconductor Quantum Dot:

Phonon-Enhanced Coherent Scattering and Off-Resonant Sideband Narrowing, Phys. Rev. Lett. **110,** 217401 (2013).

[48] D. E. Reiter, T. Kuhn, M. Glssl, and V. M. Axt, The role of phonons for exciton and biexciton generation in an optically driven quantum dot, J. Phys. Condens. Matter **26,** 423203 (2014).

[49] M. Reindl, K. D. Jöns, D. Huber, C. Schimpf, Y. Huo, V. Zwiller, A. Rastelli, and R. Trotta, Phonon-assisted two-photon interference from remote quantum emitters, Nano Lett. **17,** 4090 (2017).

[50] A. Strathearn, P. Kirton, D. Kilda, J. Keeling, and B. W. Lovett, Efficient non-Markovian quantum dynamics using time-evolving matrix product operators, Nat. Commun. **9,** 3322 (2018).

[51] S. Hepp, F. Hornung, S. Bauer, E. Hesselmeier, X. Yuan, M. Jetter, S. L. Portalupi, A. Rastelli, and P. Michler, Purcell-enhanced single-photon emission from a strain-tunable quantum dot in a cavity-waveguide device, Appl. Phys. Lett. **117,** 254002 (2020).

[52] L. Bremer, K. Weber, S. Fischbach, S. Thiele, M. Schmidt, A. Kaganskiy, S. Rodt, A. Herkommer, M. Sartison, S. L. Portalupi, P. Michler, H. Giessen, and S. Reitzenstein, Quantum dot single-photon emission coupled into single-mode fibers with 3D printed micro-objectives, APL Photonics **5,** 106101 (2020).

[53] P. Holewa, M. Burakowski, A. Musiał, N. Srocka, D. Quandt, A. Strittmatter, S. Rodt, S. Reitzenstein, and G. Sęk, Thermal stability of emission from single InGaAs/GaAs quantum dots at the telecom O-band, Sci. Rep. **10,** 21816 (2020).

[54] N. Srocka, P. Mrowiski, J. Groe, M. Schmidt, S. Rodt, and S. Reitzenstein, Deterministically fabricated strain-tunable quantum dot single-photon sources emitting in the telecom O-band, Appl. Phys. Lett. **117,** 224001 (2020).

[55] C. L. Phillips, A. J. Brash, D. P. S. McCutcheon, J. Iles-Smith, E. Clarke, B. Royall, M. S. Skolnick, A. M. Fox, and A. Nazir, Photon Statistics of Filtered Resonance Fluorescence, Phys. Rev. Lett. **125,** 043603 (2020).

[56] A. J. Brash, J. Iles-Smith, C. L. Phillips, D. P. S. McCutcheon, J. O'Hara, E. Clarke, B. Royall, L. R. Wilson, J. Mørk, M. S. Skolnick, A. M. Fox, and A. Nazir, Light Scattering from Solid-State Quantum Emitters: Beyond the Atomic Picture, Phys. Rev. Lett. **123,** 167403 (2019).

[57] E. Schöll, L. Schweickert, L. Hanschke, K. D. Zeuner, F. Sbresny, T. Lettner, R. Trivedi, M. Reindl, S. F. Covre da Silva, R. Trotta, J. J. Finley, J. Vučković, K. Müller, A. Rastelli, V. Zwiller, and K. D. Jöns, Crux of Using the Cascaded Emission of a Three-Level Quantum Ladder System to Generate Indistinguishable Photons, Phys. Rev. Lett. **125,** 233605 (2020).

[58] S. Manna, H. Huang, S. F. C. da Silva, C. Schimpf, M. B. Rota, B. Lehner, M. Reindl, R. Trotta, and A. Rastelli, Surface passivation and oxide encapsulation to improve optical properties of a single GaAs quantum dot close to the surface, Appl. Surf. Sci. **532,** 147360 (2020).

[59] V. M. Axt, T. Kuhn, A. Vagov, and F. M. Peeters, Phonon-induced pure dephasing in exciton-biexciton quantum dot systems driven by ultrafast laser pulse sequences, Phys. Rev. B **72,** 125309 (2005).

[60] S. Lüker, T. Kuhn, and D. E. Reiter, Phonon impact on optical control schemes of quantum dots: Role of quantum dot geometry and symmetry, Phys. Rev. B **96,** 245306 (2017).

[61] B. Krummheuer, V. M. Axt, T. Kuhn, I. D'Amico, and F. Rossi, Pure dephasing and phonon dynamics in GaAs- and GaN-based quantum dot structures: Interplay between material parameters and geometry, Phys. Rev. B **71,** 235329 (2005).

[62] Note that the excitation has to be resonant to the polaron shifted exciton energy, when phonons are taken into account.

[63] For resonant excitation, this value has been shown both experimentally Ding2016 and theoretically [28] to be a favorable value concerning the photonic figures of merit.

[64] C. Santori, M. Pelton, G. Solomon, Y. Dale, and Y. Yamamoto, Triggered Single Photons from a Quantum Dot, Phys. Rev. Lett. **86,** 1502 (2001).

[65] C. Santori, D. Fattal, J. Vuckovic, G. S. Solomon, and Y. Yamamoto, Indistinguishable photons from a single-photon device, Nature (London) **419,** 594 (2002).

[66] Y.-M. He, Y. He, Y.-J. Wei, D. Wu, M. Atatüre, C. Schneider, S. Höfling, M. Kamp, C.-Y. Lu, and J.-W. Pan, On-demand semiconductor single-photon source with near-unity indistinguishability, Nat. Nanotechnol. **8,** 213 (2013).

[67] Y.-J. Wei, Y.-M. He, M.-C. Chen, Y.-N. Hu, Y. He, D. Wu, C. Schneider, M. Kamp, S. Höfling, C.-Y. Lu, and J.-W. Pan, Deterministic and robust generation of single photons from a single quantum dot with 99.5% indistinguishability using adiabatic rapid passage, Nano Lett. **14,** 6515 (2014).

[68] L. Schweickert, K. D. Jöns, K. D. Zeuner, S. F. Covre da Silva, H. Huang, T. Lettner, M. Reindl, J. Zichi, R. Trotta, A. Rastelli, and V. Zwiller, On-demand generation of background-free single photons from a solid-state source, Appl. Phys. Lett. **112,** 093106 (2018).

[69] R. Hanbury Brown and R. Q. Twiss, A test of a new type of stellar interferometer on sirius, Nature (London) **178,** 1046 (1956).

[70] A. Kiraz, M. Atatüre, and A. Imamoğlu, Quantum-dot single-photon sources: Prospects for applications in linear optics quantum-information processing, Phys. Rev. A **69,** 032305 (2004).

[71] K. A. Fischer, K. Müller, K. G. Lagoudakis, and J. Vučković, Dynamical modeling of pulsed two-photon interference, New J. Phys. **18,** 113053 (2016).

[72] C. K. Hong, Z. Y. Ou, and L. Mandel, Measurement of Subpicosecond Time Intervals between Two Photons by Interference, Phys. Rev. Lett. **59,** 2044 (1987).

[73] R. Manson, K. Roy-Choudhury, and S. Hughes, Polaron master equation theory of pulse-driven phonon-assisted population inversion and single-photon emission from quantum-dot excitons, Phys. Rev. B **93,** 155423 (2016).

[74] M. Cosacchi, F. Ungar, M. Cygorek, A. Vagov, and V. M. Axt, Emission-Frequency Separated High Quality Single-Photon Sources Enabled by Phonons, Phys. Rev. Lett. **123,** 017403 (2019).

[75] H.-P. Breuer, E.-M. Laine, and J. Piilo, Measure for the Degree of Non-Markovian Behavior of Quantum Processes in Open Systems, Phys. Rev. Lett. **103,** 210401 (2009).

[76] A. Rivas, S. F. Huelga, and M. B. Plenio, Entanglement and Non-Markovianity of Quantum Evolutions, Phys. Rev. Lett. **105**, 050403 (2010).

[77] X.-M. Lu, X. Wang, and C. P. Sun, Quantum Fisher information flow and non-Markovian processes of open systems, Phys. Rev. A **82**, 042103 (2010).

[78] S. Lorenzo, F. Plastina, and M. Paternostro, Geometrical characterization of non-Markovianity, Phys. Rev. A **88**, 020102(R) (2013).

[79] Á. Rivas, S. F. Huelga, and M. B. Plenio, Quantum non-Markovianity: Characterization, quantification and detection, Rep. Prog. Phys. **77**, 094001 (2014).

[80] D. Chruścinński and S. Maniscalco, Degree of Non-Markovianity of Quantum Evolution, Phys. Rev. Lett. **112**, 120404 (2014).

[81] L. Li, M. J. Hall, and H. M. Wiseman, Concepts of quantum non-Markovianity: A hierarchy, Phys. Rep. **759**, 1 (2018).

[82] S. Wißmann, A. Karlsson, E.-M. Laine, J. Piilo, and H.-P. Breuer, Optimal state pairs for non-Markovian quantum dynamics, Phys. Rev. A **86**, 062108 (2012).

[83] W. H. Louisell, *Quantum Statistical Properties of Radiation* (Wiley, New York, 1973).

[84] H. Carmichael, *An Open Systems Approach to Quantum Optics* (Springer, Berlin, 1993).

[85] C. Roy and S. Hughes, Influence of Electron—Acoustic-Phonon Scattering on Intensity Power Broadening in a Coherently Driven Quantum-Dot—Cavity System, Phys. Rev. X **1**, 021009 (2011).

[86] A. Nazir and D. P. S. McCutcheon, Modelling exciton-phonon interactions in optically driven quantum dots, J. Phys. Condens. Matter **28**, 103002 (2016).

[87] J. Iles-Smith and A. Nazir, Quantum correlations of light and matter through environmental transitions, Optica **3**, 207 (2016).

[88] D. Englund, B. Shields, K. Rivoire, F. Hatami, J. Vučković, H. Park, and M. D. Lukin, Deterministic coupling of a single nitrogen vacancy center to a photonic crystal cavity, Nano Lett. **10**, 3922 (2010).

[89] K. Beha *et al.*, Diamond nanophotonics, Beilstein J. Nanotechnol. **3**, 895 (2012).

[90] I. Aharonovich, D. Englund, and M. Toth, Solid-state single-photon emitters, Nat. Photonics **10**, 631 (2016).

[91] K. G. Fehler, A. P. Ovvyan, N. Gruhler, W. H. P. Pernice, and A. Kubanek, Efficient coupling of an ensemble of nitrogen vacancy center to the mode of a high-Q, Si_3N_4 photonic crystal cavity, ACS Nano **13**, 6891 (2019).

[92] E. Janitz, M. K. Bhaskar, and L. Childress, Cavity quantum electrodynamics with color centers in diamond, Optica **7**, 1232 (2020).

[93] P. P. J. Schrinner, J. Olthaus, D. E. Reiter, and C. Schuck, Integration of diamond-based quantum emitters with nanophotonic circuits, Nano Lett. **20**, 8170 (2020).

[94] J. C. Lee, I. Aharonovich, A. P. Magyar, F. Rol, and E. L. Hu, Coupling of silicon-vacancy centers to a single crystal diamond cavity, Opt. Express **20**, 8891 (2012).

[95] K. G. Fehler, A. P. Ovvyan, L. Antoniuk, N. Lettner, N. Gruhler, V. A. Davydov, V. N. Agafonov, W. H. Pernice, and A. Kubanek, Purcell-enhanced emission from individual SiV- center in nanodiamonds coupled to a Si_3N_4-based, photonic crystal cavity, Nanophotonics **9**, 3655 (2020).

[96] N. V. Proscia, H. Jayakumar, X. Ge, G. Lopez-Morales, Z. Shotan, W. Zhou, C. A. Meriles, and V. M. Menon, Microcavity-coupled emitters in hexagonal boron nitride, Nanophotonics **9**, 2937 (2020).

[97] J. E. Fröch, S. Kim, N. Mendelson, M. Kianinia, M. Toth, and I. Aharonovich, Coupling hexagonal boron nitride quantum emitters to photonic crystal cavities, ACS Nano **14**, 7085 (2020).

[98] S. Rodt, S. Reitzenstein, and T. Heindel, Deterministically fabricated solid-state quantum-light sources, J. Phys. Condens. Matter **32**, 153003 (2020).